# Preparation and Adsorption Performance of Starch Microspheres Towards $Cu^{2+}$, $Co^{2+}$, and $Ni^{2+}$

Zhongjin Li[1*], Zongcheng Miao[1], Lei Wang[1], Jiegen Liu[1], Yan Dai[2] and Wenxue Bai[2]

(1) College of Chemistry and Chemical Engineering, Shaan-xi University of Science and Technology, Xi-an, Shaan-xi, 710021, PR China
(2) Xi-an Ruilian Modern Electronic Chemicals Co. Ltd., Xi-an Shaan-xi, 710061, PR China

## A B S T R A C T

Cross-linking starch microsphere (CSM) is a derivative of crude starch and has been studied and applied widely in the fields of medicine and sanitary devices. In our studies we have found that starch microsphere has good adsorption performance to metal ions in water. In this work, a type of cross-linking starch microsphere has been synthesized by reversed phase suspension method using soluble starch as raw material with *N,N'*-methylenebisacrylamide as a cross-linking agent. The observation through scanning electron microscopy (SEM) shows that CSM is a homogeneous mixture of spherical particulates with heterogeneous surface with particles' average diameter of about 50 $\mu$m. The structure characteristics of carbonyl group and second acylamide in Fourier transform infrared spectroscopy spectrogram of CSM demonstrates that the soluble starch is definitely cross-linked with *N,N'*-methylenebisacrylamide. The synthetic analysis of X-ray diffraction indicates that the cross-linking function decreases the crystallinity of CSM compared with that of soluble starch. The adsorption capacity of CSM towards $Cu^{2+}$, $Co^{2+}$, and $Ni^{2+}$ increases with the increase in metal ion concentration, and by lowering the temperature, adsorption can be accelerated. The adsorption behaviour of CSM in different temperatures is in agreement with the Freundlich isothermal equation. The research results show that the adsorption process is exothermic, can proceed spontaneously, with the adsorption force mainly derived from enthalpy changes. The thermodynamic parameters of adsorption process show that the adsorption behaviour of CSM towards $Cu^{2+}$, $Co^{2+}$, and $Ni^{2+}$ is of a physical type.

(∗) To whom correspondence to be addressed.
E-mail: 04miaozongcheng@sust.edu.cn

## INTRODUCTION

Starch is a kind of natural polymer with good degree of biodegradability. Now researchers are focusing their attention to modify starch to synthesize functional polymers [1,2] which would be used in the fields of wastewater treatment and heavy metal enrichment and recovery [3-5]. Starch microsphere is an artificial starch derivative and can be synthesized by cross-linking reaction from crude and modified starches. Starch microspheres have been used successfully in nasal drug delivery system, artery embolization studies, radiotherapy, immuno-assay, etc. [6,7]. The microsphere is novel as an adsorp-

tive material [8] with tremendous development potential, because of its irregular appearance, uniform size, suitable swelling, three-dimensional network structure, suitable shell/pore diameter, specific surface area, and good mechanical strength. Starch microsphere is a novel material in the field of absorbency and separation of harmful metal ions or wastewater treatment process for its biocompatibility and biodegradability properties, and it does not cause any secondary pollution to environment. Thus, it is very important to prepare starch microsphere with suitable methods and to study the adsorption thermodynamics towards metal ion, followed by the study of adsorption mechanism towards metal ions as an important work.

In this research work, a new type of cross-linkling starch microsphere (CSM) by $N,N'$-methylenebisacrylamide was synthesized via reversed phase suspension method [9] with starch as soluble material. For $N,N'$-methylenebisacrylamide in cross-linking the modified starch, the chelating functional groups added to the microspheres' structure, are sites that the metal ions can be adsorbed on microspheres more easily. Based on the study of past several years, we have elucidated the cross-linking mechanism between the starch and $N,N'$-methylenebisacrylamide. In the reversed phase suspension system, soluble starch, $N,N'$-methylenebisacrylamide, $K_2S_2O_8$, and $Na_2SO_3$ are dissolved in water, and then small water droplets are formed in the polymerization reaction cell. The cross-linking reaction starts by the generation of the free radical $SO_4^{-}\cdot$ ($SO_3^{-}\cdot$), and then $SO_4^{-}\cdot$ ($SO_3^{-}\cdot$) which react with amylose to give starch free radicals [10].

Amylose is a linear polymer, exhibiting right-handed helix structures, composed of $\alpha$-D-starch linked with $\alpha$-D-1,4 glycosidic bonds, which contains six glucose units. There are only hydrogen atoms in the interior section of helix structures which are hydrophobic, while the hydroxyl groups located on the exterior are hydrophilic. Thus, the cross-linking reaction will proceed not only between the different glucose units in the same starch molecules but also between the different starch molecules in the same liquid droplet. When the polymerization reaction is initiated, the cross-linking may occur in all possible positions, and in the presence of low molecular weight free radical it will be more favoured to the exterior cross-linking reaction of starch molecules.

With higher degree of cross-linking, the interaction in chain link of the interior of starch molecule increased which makes the polymer morphology more tight in forming new microspheres with three-dimensional network structure, and then the microspheres separate out from the water phase. Due to cross-linking, the water molecule has been extracted from starch molecules during the microsphere generation, and micro channels substitute water molecules in the interior part of microsphere to generate pores.

This kind of CSM has good adsorption properties for its larger effective surface[11,12], suitable pore volume[13] and more active groups[14,15]. The study on the adsorption behaviour of CSM towards $Cu^{2+}$, $Co^{2+}$ and $Ni^{2+}$ would develop the application arena of CSM to the fields of wastewater treatment, cation-exchange resin, supported metal catalyst, etc.

This research has explored the adsorption thermodynamic behaviour of CSM towards metal ions and it provides theoretical basis for further application of CSM.

## EXPERIMENTAL

### Materials and Reagents
Soluble starch was purchased from Junle Chemical Works (Peng-zhou, Si-Chuan Province, China) with molecular weight range between 32000 and 160000 g/mol. Cyclohexane, chloroform, sodium hydroxide, ethyl acetate, acetone, absolute alcohol, Span60, Tween60, $K_2S_2O_8$, $Na_2SO_3$, $N,N'$-methylenebisacrylamide, $CuSO_4\cdot5H_2O$, $CoCl_2\cdot6H_2O$ and $NiSO_4\cdot 6H_2O$, all reaction reagents are analytical and they have been used without further purification. In all experiments distilled water was used.

The surface morphology of CSM was observed by scanning electron microscopy (Model JSM-6460, Electronics Enterprise, Japan). The elemental composition of the surface layer of CSM was analyzed using X-ray diffractometer (Model D/max-2200 pc, Rigaku, Japan). The characteristic groups of CSM was characterized using Fourier transform infrared spectroscopy (Model VECTOR-22, Bruker, German). The concentration of metal ion was measured using atomic absorption spectrophotometer (Model AA-6800, Shimadzu, Japan).
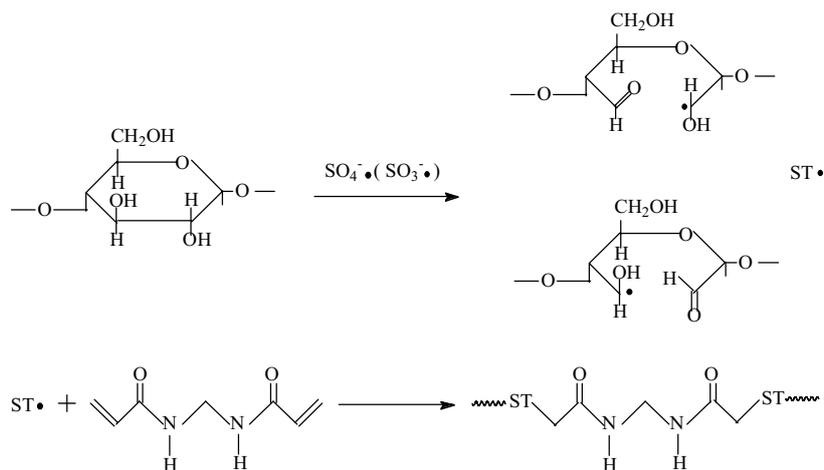
**Scheme I.** The synthesis of CSM.

## CSM Characterizations

As it is evident in Figure 1, the average particle size of CSM is about 50 μm, and CSM is a spherical particulate with irregular porous surface, and displays a homogeneous and dense structure. In the synthesis process, the force between chain links of starch molecules increased during cross-linking. Thus, the molecular structure became more compact, ultimately produced microspheres with spatial reticular structure and precipitated from water phase. The internal water molecules in the microsphere were exuded, thus, many microtunnels were left which could allow metal ions reaching the interior section of the porous microsphere to achieve quick adsorption.

## Preparation of CSM

CSM was obtained using a three-necked flask provid-ed with an anchor type stirrer, a digital temperature indicating/controlling instrument and a reflux condenser. The flask was maintained at a constant temperature with thermostatic water bath. In detail, 2 g of soluble starch was dissolved in 20 mL distilled water under stirring, regulating the pH to 8. The temperature of soluble starch solution was kept at 80°C for 30 min in order to make the starch dissolve completely, and then depressed to 50°C. The solution was added to 100 mL dispersion medium (80 mL cyclohexane and 20 mL chloroform) in which 1 g of Span60-Tween60 as dispersion agent was dissolved at 50°C under reflux. The obtained W/O emulsion was stirred for 30 min and then the emulsification effect was checked up. After the air was ejected completely from the three-necked flask by nitrogen flow, 0.2 g of *N,N'*-methylenebisacrylamide dissolved in chloroform and
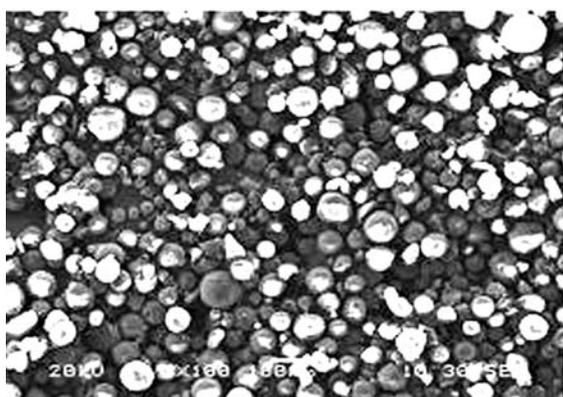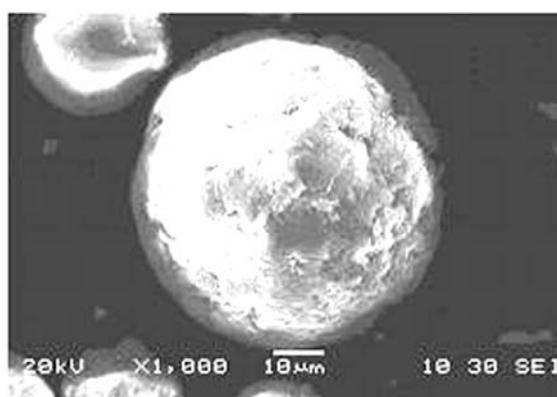


Figure 1. SEM micrographs of starch microspheres: (a) magnification ×100 and (b) magnification ×1000.

0.04 g of $K_2S_2O_8$ and 0.03 g $Na_2SO_3$ were added. The cross-linking reaction was carried out for 2 h at 50°C. The cross-linked starch microspheres were recovered by centrifugal separation. The residuals were removed by washing the microspheres in the following order with organic solvent, ethyl acetate, acetone, and anhydrous ethanol. Then, microspheres were dried completely, and the mass and the yield were 1.06 g and 48.2%, respectively. The colour of CSM prepared as reported above was whitish to pale yellow, containing no impurities.

**Mensuration of Adsorption Isotherm**
The adsorption experiment was carried out in 250 mL Erlenmeyer flasks equipped with stoppers, in which 0.5000 g of CSM and various different concentrations of $Cu^{2+}$, $Co^{2+}$, or $Ni^{2+}$ aqueous solution were added each in a separate flask. The Erlenmeyer flasks were placed in constant temperature bath for 12 h, controlling the temperature at 298 K, 308 K and 318 K, respectively [16,17]. The absorbance of solutions was determined by atomic absorption spectrophotometer. The equilibrium adsorption capacity was calculated according to the following equation.

$$Q_e = \frac{V(C_0 - C_e)}{m} \tag{1}$$

where $Q_e$, $C_0$, $C_e$, V, and m are the equilibrium adsorption capacity (mmol/g), the initial concentration of metal ion (mmol/L), the equilibrium concentration (mmol/L), the solution volume (L), and the mass of CSM (g), respectively.

**RESULTS AND DISCUSSION**

**Structure Analysis of CSM**
Figure 2 shows comparative FTIR spectrograms of CSM and soluble starch (ST). It shows clearly that the characteristic peaks at 3445 cm$^{-1}$ (CSM) and 3443 cm$^{-1}$ (ST), namely, the strong and wide absorption bands of stretching vibration of hydroxyl group are attributed to the cross-linking reaction which not only results in weakening the association between hydrogen bonds but also makes the absorption peak of CSM to become more lanky and shift slightly to
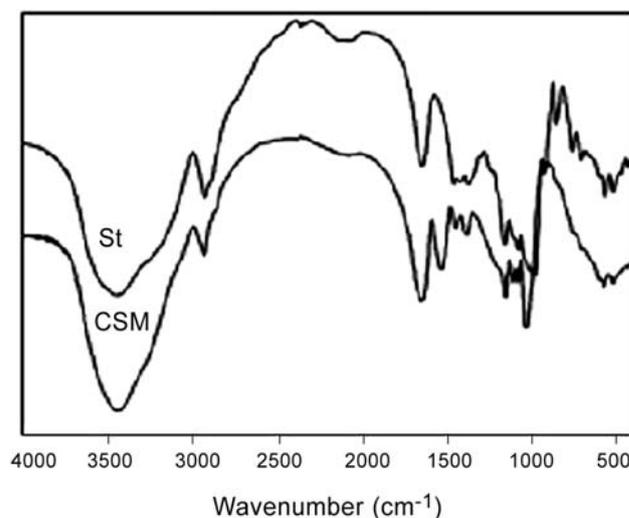


**Figure 2.** FTIR spectra of soluble starch and CSM.

high frequency regions. The absorption peaks at 2928 cm$^{-1}$ belong to the stretching vibration of C-H bonds of glucose units which verifies that the basic structural units of starch are not markedly changed for the formation of cross-linking bonds in CSM structure. The peaks at 1154 cm$^{-1}$ and 1109 cm$^{-1}$ are related to asymmetry and symmetry vibrations of C-O-C, respectively. It is very important that the peaks presented at 1652 cm$^{-1}$ and 1538 cm$^{-1}$ proved structure characteristics of carbonyl group and acylamide, respectively. Overall, it can be deduced logically that the soluble starch has definitely cross-linked with N,N'-methylenebisacrylamide.

**Physical Properties of CSM by XRD**
Figure 3 displays the analytical results of X-ray diffraction of the soluble starch and CSM. The sharp diffraction peaks at 16.8°, 20°, 22.4° and 23.6° of 2θ are presented in spectrogram of soluble starch, and the crystallinity is about 33%. In spectrogram of CSM, relative intensity of the diffraction peak at 20° reduces obviously and its range becomes correspondingly wide due to the decreased crystallinity while the peaks at 16.8°, 22.4°, and 23.6° completely disappear. The weaker diffraction peaks at 14.6°, 29.3°, and 31.6° appear simultaneously in the spectrogram of CSM, and crystallinity is about 6.4%. In view of these data, it can be concluded that these changes are involved in the cross-linking reaction which made intermolecular force and hydrogen bond weaken
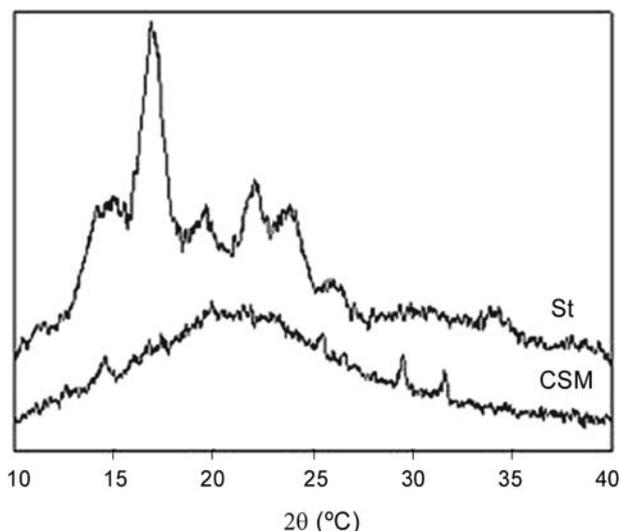
**Figure 3.** XRD patterns of soluble starch and CSM.



**Figure 5.** Adsorption isotherm of $Co^{2+}$.

between the chains of starch molecules. Thus, the regularity of starch molecules was lost and crystallization capacity was reduced as well.

**Isothermal Adsorption Curves of CSM Towards $Cu^{2+}$, $Co^{2+}$, and $Ni^{2+}$**

Figures 4-6 are the isothermal adsorption curves of $Cu^{2+}$, $Co^{2+}$, and $Ni^{2+}$ on CSM at 298 K. The experimental results show that the adsorption capacity of CSM increases rapidly with the increasing of ion concentration. But when the metal ion concentration increased to a certain extent, the increasing trend of saturated adsorption capacity became slower. Also, it can be explained that at same concentration the
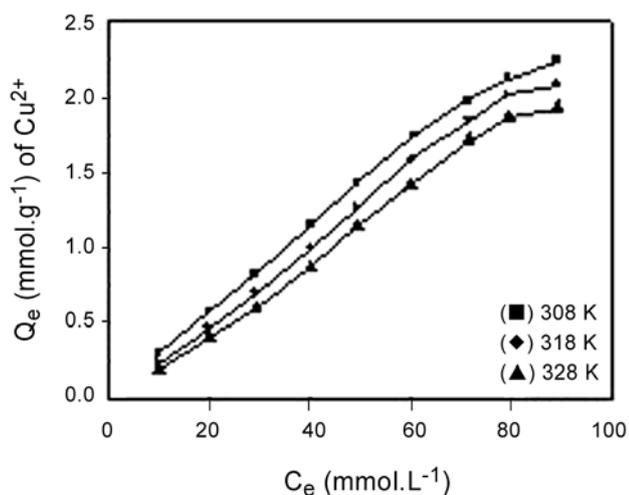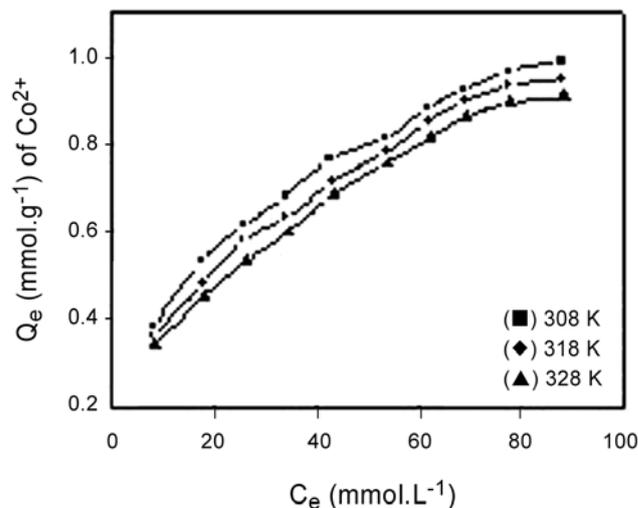
temperature is lower, and the adsorption capacity of CSM is more enhanced. This is mainly because the energy of metal ion decreases with temperature decreasing, and as a result the adsorption of CSM to $Cu^{2+}$, $Co^{2+}$, and $Ni^{2+}$ is an exothermal process. We can conclude that the saturated adsorption capacity of CSM towards $Cu^{2+}$ is the highest, 2.30 mmol/g, then $Co^{2+}$, 1.17 mmol/g, and the least is $Ni^{2+}$ with 0.97 mmol/g. Thus, the coordination adsorption capacities of CSM towards the metal ions are $Cu^{2+}$, $Co^{2+}$ and $Ni^{2+}$ in turn.

The isothermal adsorption curve can be approximately expressed as a mathematical equation when it obeys an adsorption model. In other words, it is
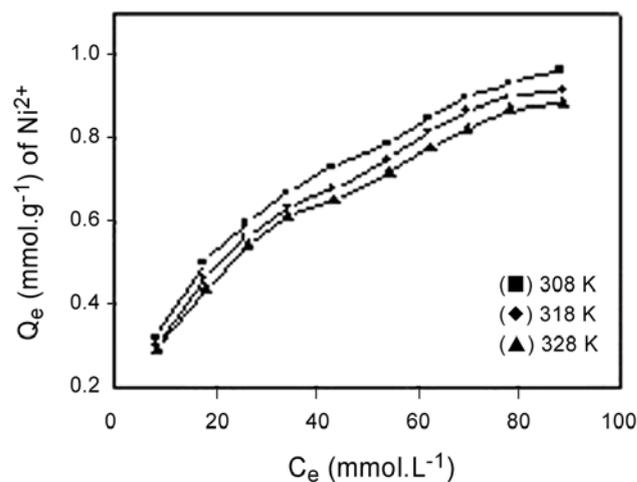


**Figure 4.** Adsorption isotherm of $Cu^{2+}$.



**Figure 6.** Adsorption isotherm of $Ni^{2+}$.

**Table 1.** Equations of adsorption of $Cu^{2+}$ and $Co^{2+}$ at different temperatures.

| Model | T (K) | Adsorption towards $Cu^{2+}$ | | Adsorption towards $Co^{2+}$ | |
|---|---|---|---|---|---|
| | | Equations | R | Equations | R |
| Langmuir | 308 | $C_e/Q_e=0.11079C_e+0.02532$ | 0.9902 | $C_e/Q_e=0.40441C_e+0.00736$ | 0.9575 |
| | 318 | $C_e/Q_e=0.01342C_e+0.02467$ | 0.9907 | $C_e/Q_e=0.365C_e+0.00739$ | 0.9659 |
| | 328 | $C_e/Q_e=0.03869C_e+0.02339$ | 0.9914 | $C_e/Q_e=0.33438C_e+0.00728$ | 0.9669 |
| Freundlich | 308 | $Q_e=0.04642C_e^{0.87154}$ | 0.9916 | $Q_e=0.16865C_e^{0.39936}$ | 0.9974 |
| | 328 | $Q_e=0.02908C_e^{0.96306}$ | 0.9913 | $Q_e=0.14449C_e^{0.42607}$ | 0.9948 |
| | 328 | $Q_e=0.02068C_e^{1.02294}$ | 0.9908 | $Q_e=0.12738C_e^{0.44532}$ | 0.9932 |

possible that the correlation between the equilibrium concentration ($C_e$) obtained from experiments and the equilibrium adsorption capacity ($Q_e$) would accord with certain mathematical formula. Actually, the Langmuir equation and Freundlich equation are the most usual calculation formulae for experimental data of liquid phase adsorption if the sorption of solvent is neglected. Commonly, the verification of linear relationship by substituting the experimental data into eqn (2) is the way to estimate whether they truly obey Langmuir model.

$$C_e/Q_e = C_e/Q_m + 1/(Q_m b) \tag{2}$$

where $Q_e$, $Q_m$, $b$, $C_e$ are the equilibrium adsorption capacity of metal ion on CSM (mmol/g), the saturated adsorption capacity (mmol/g), the adsorption equilibrium constant, and the equilibrium concentration of metal ion in the solution (mmol/L), respectively.

In the same way, the confirmation of linear rela-

tionship of eqn (3) by substitution method is the way to evaluate whether the experimental data fit the Freundlich model.

$$ln Q_e = ln K_F + \frac{1}{n} \times ln C_e \Rightarrow Q_e = K_F \times C_e^{\frac{1}{n}} \tag{3}$$

where $Q_e$, $C_e$, $K_F$, and $1/n$ are the equilibrium adsorption capacity of metal ion on CSM (mmol/g), the equilibrium concentration of metal ion in the solution (mmol/L), and the adsorption constants, respectively.

The experimental data were calculated with the regression analysis according to eqns (2) and (3), and the results are listed in Tables 1 and 2.

It can be seen from Tables 1 and 2 that the adsorption model of CSM towards $Cu^{2+}$, $Co^{2+}$, and $Ni^{2+}$ agrees well with the Freundlich isothermal equation relative to the Langmuir isothermal equation, and therefore the adsorption behaviour is more easily explained [18].

**Table 2.** Equations of adsorption $Ni^{2+}$ at different temperatures.

| Model | T (K) | Adsorption towards $Cu^{2+}$ | |
|---|---|---|---|
| | | Equations | R |
| Langmuir | 308 | $C_e/Q_e=0.36007C_e+0.00759$ | 0.9431 |
| | 318 | $C_e/Q_e=0.33234C_e+0.00739$ | 0.9478 |
| | 328 | $C_e/Q_e=0.31536C_e+0.00711$ | 0.9515 |
| Freundlich | 308 | $Q_e=0.14059C_e^{0.43504}$ | 0.9934 |
| | 328 | $Q_e=0.12636C_e^{0.44894}$ | 0.9929 |
| | 328 | $Q_e=0.11851C_e^{0.4538}$ | 0.9937 |

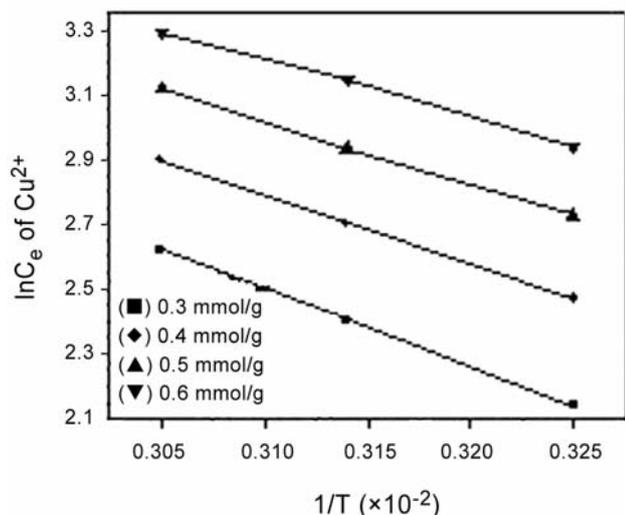**Figure 7.** Influence of temperature on distribution ratio for $Cu^{2+}$.



**Figure 8.** Influence of temperature on distribution ratio for $Co^{2+}$.

## Adsorption Thermodynamic Properties of CSM Towards $Cu^{2+}$, $Co^{2+}$, and $Ni^{2+}$

### Adsorption Enthalpy

There is a close relationship between adsorption enthalpy and adsorption quantity. The adsorption enthalpy is derived from a certain adsorption quantity, so it is referred as "equivalent adsorption enthalpy" (EAE). The Clausius-Clapeyron equation can be used to calculate the EAE [19].

$$\ln C_e = \Delta H / RT + \ln K_0 \qquad (4)$$

where R, T, $C_e$, and $K_0$ are the gas constant (8.314 J/k.mol), the absolute temperature (K), the adsorption equilibrium concentration in the temperature T (mmol/g), and the adsorption constant, respectively. $C_e$ would be obtained through Freundlich equation as $Q_e$ has changed within the range 0.3-0.6 mmol/g at different temperatures of 308 K, 318 K or 328 K.

In Figures 7-9, the influence of temperature on distribution ratio as to $Cu^{2+}$, $Co^{2+}$ and $Ni^{2+}$ are shown. According to these curves it can be deduced that the correlated coefficients are all greater than 0.99, thus, the hypothesis that $\Delta H$ is being unrelated to the temperature sounds reasonable in a process with a certain working temperature range. The $\Delta H$ at different adsorption quantities could be calculated, according to the slope of the curve and the data are listed in Tables 3-5.
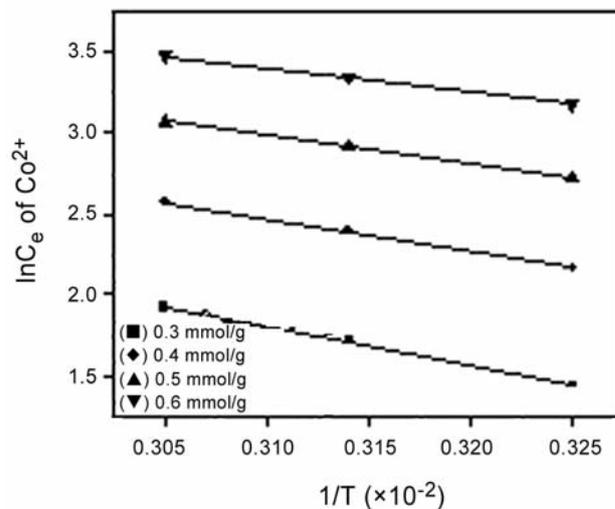
The properties of adsorption force were reflected directly by thermodynamic parameters of adsorption enthalpy. The value of adsorption enthalpy $\Delta H$ of CSM adsorbed $Cu^{2+}$, $Co^{2+}$ or $Ni^{2+}$ is negative, and it declares that the adsorption process is exothermic, and the lower temperature can accelerate the adsorption. The adsorption process depends on the interaction between adsorbates and adsorbents, different acting forces releasing different amounts of heat. The adsorption enthalpy, however, is the result of these factors, as the value of $\Delta H$ depends on the competition results of total exothermic and endothermic
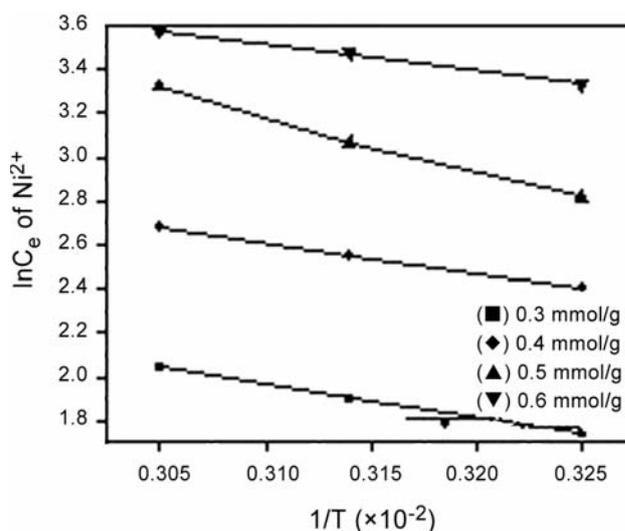


**Figure 9.** Influence of temperature on distribution ratio for $Ni^{2+}$.

**Table 3.** Thermodynamic properties of the systems tested adsorption $Cu^{2+}$.

| $Q_e$ (mmol/g) | $\Delta H$ (kJ/mol) | $\Delta G$ (kJ/mol) | | | $\Delta S$ (J/mol·K) | | |
|---|---|---|---|---|---|---|---|
| | | 308 (K) | 318 (K) | 328 (K) | 308 (K) | 318 (K) | 328 (K) |
| 0.3 | -20.045 | | | | -55.540 | -54.400 | -52.984 |
| 0.4 | -17.850 | -2.938 | -2.745 | -2.666 | -48.414 | -48.127 | -46.292 |
| 0.5 | -16.252 | | | | -43.225 | -42.472 | -41.420 |
| 0.6 | -14.966 | | | | -39.050 | -38.430 | -37.499 |

effects. As to the adsorption system, the total exothermic effect belongs to desorption heat of the solute which is bigger than the solvent, thus, this adsorption process is exothermic.

$\Delta H$ decreases slightly with the increasing value of $Q_e$, probably due to the inhomogeneity of the CSM surface. When metal ion has lower concentration, adsorbate always occupies the absorption sites, which has lower energy for CSM uneven surface [20]. Following the increasing of adsorption quantity, the CSM surface is covered gradually and the pores are filled, the interaction between adsorbate and absorbent is then substituted by the interaction between the adsorbate on CSM and in the aqueous solution, leading to the direct result of decreased adsorption enthalpy.

*Adsorption Free Energy*
The value of adsorption free energy, $\Delta G$, can be calculated by Gibbs equation [21].

$$\Delta G = -RT \int_0^x Q_e dx / x \qquad (5)$$

where x is mole fraction of the adsorbate in the aqueous solution. The Freundlich isothermal adsorption equation is used to derive the equation that the unit free energy change is unrelated to $Q_e$.

$$\Delta G = -nRT \qquad (6)$$

where n is the coefficient of Freundlich isothermal adsorption equation, and it is considered to relate to the adsorption driving force between adsorbate and adsorbent.

The adsorption free energy $\Delta G$ at different conditions of CSM adsorption towards $Cu^{2+}$, $Co^{2+}$ and $Ni^{2+}$ have been listed in Tables 3-5. The adsorption free energy $\Delta G$ has been expressed by adsorption driving force and favourable adsorption based on the thermodynamics. As $\Delta G$s are all negative values, it shows that the adsorption has proceeded spontaneously, the adsorbate is apt to be adsorbed on the CSM surface from aqueous solution. With the increase in temperature, the absolute value of $\Delta G$ increased indicating that the spontaneous adsorption process is stimulated at higher temperature, although the trend is relatively small which is related to the entropy compensation. The relationship of enthalpy to $\Delta G$ is opposite to that of entropy, but the complications exist, and the microcosmic complication is related to intermolecular

**Table 4.** Thermodynamic properties of the systems tested adsorption $Co^{2+}$.

| $Q_e$ (mmol/g) | $\Delta H$ (kJ/mol) | $\Delta G$ (kJ/mol) | | | $\Delta S$ (J/mol·K) | | |
|---|---|---|---|---|---|---|---|
| | | 308 (K) | 318 (K) | 328 (K) | 308 (K) | 318 (K) | 328 (K) |
| 0.3 | -20.234 | | | | -44.878 | -44.117 | -43.020 |
| 0.4 | -17.106 | -6.412 | -6.205 | -6.124 | -34.722 | -34.281 | -33.484 |
| 0.5 | -14.681 | | | | -26.846 | -26.652 | -26.088 |
| 0.6 | -12.698 | | | | -20.410 | -20.419 | -20.044 |

**Table 5.** Thermodynamic properties of the systems tested adsorption $Ni^{2+}$.

| $Q_e$ (mmol/g) | $\Delta H$ (kJ/mol) | $\Delta G$ (kJ/mol) | | | $\Delta S$ (J/mol·K) | | |
|---|---|---|---|---|---|---|---|
| | | 308 (K) | 318 (K) | 328 (K) | 308 (K) | 318 (K) | 328 (K) |
| 0.3 | -12.784 | | | | -22.397 | -21.683 | -20.656 |
| 0.4 | -11.637 | -5.886 | -5.889 | -6.009 | -18.670 | -18.074 | -17.157 |
| 0.5 | -21.209 | | | | -49.750 | -48.491 | -46.341 |
| 0.6 | -10.029 | | | | -13.450 | -13.018 | -12.255 |

forces and degree of freedom in molecular movements.

*Adsorption Entropy Changes*
The adsorption entropy change $\Delta S$ can be calculated by Gibbs equation [22]:

$$\Delta S = \frac{\Delta H - \Delta G}{T} \qquad (7)$$

The values of entropy changes of adsorption process are shown in Tables 3-5. It shows that the values of $\Delta S$ are all negative; for the adsorbate, molecular movement has been restricted to the surface of CSM. From the value of $\Delta S$, it can be seen that enthalpy is the main adsorption driving force.

## CONCLUSION

The cross-linked starch microspheres with irregular porous surface were successfully obtained by chemical cross-linking by inverse suspension system. The average particle size of CSM was about 50 μm, and the adsorption capacity of CSM towards metal ion has been studied. This has indicated that the adsorption capacity of CSM increases with the increasing of metal ion concentration and at the same concentration, lower temperature would favour greater adsorption.

The adsorption behaviour of CSM towards $Cu^{2+}$, $Co^{2+}$ and $Ni^{2+}$ at different temperatures agreed far better with Freundlich isothermal equation. Since the values of adsorption enthalpies are all negative, it shows that the adsorption process is exothermic, and at lower temperature adsorption becomes more

favourable. The values of adsorption energies are also negative, and as a result the adsorption can proceed spontaneously. The adsorption driving force comes mainly from the enthalpy changes.

The thermodynamic parameters of adsorption process shows that the adsorption behaviour of CSM toward $Cu^{2+}$, $Co^{2+}$ and $Ni^{2+}$ belongs to physical type of adsorption, and this study has provided the theoretical basis for CSM to be applied in adsorption systems, such as wastewater treatment, ion exchange, supported catalyst, etc.

## REFERENCES

1. Nikazar M, Safari B, Bonakdarpour B, Milani Z, Improving the biodegradability and mechanical strength of corn starch-LDPE blends through formulation modification, *Iran Polym J*, **14**, 1050-1057, 2005.
2. Ghafoori M, Mohammadi N, Ghaffarian SR, Resistance-to-flow analysis in low density polyethylene/plasticized starch blends containing compatibilizers with attractive and repulsive interactions, *Iran Polym J*, **15**, 747-755, 2006.
3. Gu R, Sun Y, Wang C, Syntheses and properties of new spherical amino-starch resins, *Chin J Mater Res*, **15**, 473-478, 2001.
4. Dong Y, Lu J, Synthesis of starch-*g*-polyviny-

lamine and its absorption property, *J Chem Eng Chin Uni*, **19**, 65-70, 2005.

5.  Zhang Y, Chen J, Feng Q, Yan X, Study on the synthesis of adsorbent and adsorption ability of dual-modified starch, *Ion Exch Adsorpt*, **22**, 77-83, 2006.

6.  Suzuki M, Nagata K, Masunaga S, Kinashi Y, Sakurai Y, Maruhashi A, Ono K, Biodistribution of [10]B in a rat liver tumor model following intra-arterial administration of sodium borocaptate (BSH)/degradable starch microspheres (DSM) emulsion, *App Radia Iso*, **61**, 933-937, 2004.

7.  Mundargi RC, Shelke NB, Rokhade AP, Patil SA, Aminabhavi TM, Formulation and in-vitro evaluation of novel starch-based tableted microspheres for controlled release of ampicillin, *Carbohydr Polym*, **71**, 42-53, 2008.

8.  Yuan J, Chen Y, Tang X, Shen S, Application of modified starches to environmental and biochemical engineering, *Chem Ind Eng Pro*, 23, 1312-1315, 2004.

9.  Wang L, Li ZJ, Zhao XF, Lai XJ, Preparation and characterization of starch microspheres as drug-carrier, *Fine Chem*, **24**, 86-90, 2007.

10. Xie C, Yang L, Gao Q, Preparing starch nano-spheres by inverse microemulsion polymerization and its application in biomedicine, *Mod Chem Ind*, **24**, 62-65, 2004.

11. Pena M, Meng X, Korfiatis GP, Jing C, Adsorption mechanism of arsenic on nanocrystalline titanium dioxide, *Environ Sci Technol*, **40**, 1257-1262, 2006.

12. Liu X, Lu X, Hoa Q, Lu Z, Yang K, Wang R, Xu S, A new integrated method for characterizing surface energy heterogeneity from a single adsorption isotherm, *J Phys Chem B*, **109**, 15828-15834, 2005.

13. Calleja G, Coto B, Pinar A, Morales-Cas A M, Ethane adsorption in slit-shaped micropores: Influence of molecule orientation on adsorption capacity, *Adsorption*, **12**, 45-54, 2006.

14. Hiradata S, Furubayashi A, Uchida N, Fujii Y, Adsorption of 2, 4-dichlorophenoxyacetic acid by an andosol, *J Environ Qual*, **36**, 101-109, 2007.

15. Sun Y, Chen JL, Li AM, Liu F-Q, Zhang QX, Adsorption of phenol from aqueous solution by aminated hypercrosslinked polymers, *Adsorpt Sci*

*Technol*, **23**, 335-345, 2005.

16. An JH, Dultz S, Adsorption of tannic acid on chitosan montmorillonite as a function of pH and surface charge properties, *Appl Clay Sci*, **36**, 256-264, 2007.

17. Coelho TC, Laus R, Mangrich AS, de Fávere VT, Laranjeira MCM, Effect of heparin coating on epichlorohydrin cross-linked chitosan microspheres on the adsorption of copper (II) ions, *React Funct Polym*, **67**, 468-475, 2007.

18. He BL, Wang WQ, *Resin Ion Exchange Adsorption*, Shang-hai Scientific and Technological Education Publishing, Shang-hai, 1995.

19. Cao YX, Zhang C, Ping QN, Preparation and characterization of a novel poly (*N*-isopropyl acrylamide)-chitosan, *Polym Mater Sci Eng*, **21**, 236-239, 2005.

20. Carter MC, Kilduff JE, Weber Jr WJ, Site energy distribution analysis of preloaded adsorbents, *Environ Sci Technol*, **29**, 1773-1780, 1995.

21. Garcia-Delgado RA, Cotoruelo-Minguez LM, Rodriguez JJ, Equilibrium study of single-solute adsorption of anionic surfactants with polymeric XAD resins, *Sep Sci Technol*, **27**, 975-987, 1992.

22. Fu XC, Shen WX, Yao TY, *Physical Chemisty*, 4th ed, High Education, Beijing, 1990.